

Intertwined effects of elastic deformation and damage on vortex pinning and J_c degradation in polycrystalline superconductors

Qing-Yu Wang¹, Shuai Hu², You-He Zhou³, Cun Xue^{2,*}

¹*School of Aeronautics, Northwestern Polytechnical University, Xi'an 710072, China*

²*School of Mechanics, Civil Engineering and Architecture, Northwestern Polytechnical University, Xi'an 710072, China*

³*Department of Mechanics and Engineering Sciences, College of Civil Engineering and Mechanics, Lanzhou University, Lanzhou 730000, China*

xuecun@nwpu.edu.cn

Abstract

The damage and the critical current density (J_c) degradation of polycrystalline superconductors induced by strain dramatically influence their performance in applications. Unfortunately, the state-of-the-art experimental techniques are unable to detect the damage of internal polycrystalline structures and the microscopic superconductivity in the presence of strain. We propose a groundbreaking multi-scale theoretical framework aimed at revealing the underlying physical mechanisms of the reversible and irreversible J_c degradation induced by the strain through tackling the complex intertwined effects of elastic deformation and damage on the superconductivity of grain boundaries and the associated vortex pinning. The results are well validated by experimental measurements. Utilizing the benchmarked physical model, we demonstrate that the damage evolutions of polycrystalline superconductors in the presence of strain can be approximately estimated by means of the electromagnetic experiments on J_c . Furthermore, we also discuss the characteristics of damage and J_c degradation of polycrystalline superconductors subjected to biaxial mechanical loads. The findings will pave the way to investigate the tunable vortex pinning and J_c of superconductors by strain, and to develop a brand new electromagnetic method to manifest the damage of polycrystalline superconductors.

Main text—Mechanical loads such as Lorentz force and thermal stress can lead to damages and critical property degradations of superconductors, seriously threatening applications of superconducting devices. The plastic deformation, filament breakage, and even catastrophic destruction of superconductors were observed in numerous experiments [1-3]. For superconducting thin films, the damage evolution can be directly observed by

scanning electron microscope (SEM) or transmission electron microscope (TEM). More recently, Zhou et al [4] pioneered the application of magneto-optical imaging (MOI) to observe the strain-induced damage evolution in coated conductors at macroscale, shedding light on the origins of initial damage. However, for polycrystalline superconductors like Nb₃Sn wire consisting of a copper matrix and thousands of filaments [5], the damage of internal polycrystalline structures are unable to be detected by the state-of-the-art experimental techniques.

Moreover, due to the strain sensitivity of polycrystalline superconductors such as Nb₃Sn [6, 7], the typical loss of critical current (I_c) with intrinsic axial-strain $\epsilon_a=0.40\%$ at 4.07 K is about 40% [8], thereby reducing its quench current threshold and bringing about challenge to its safe and stable operation [9]. Revealing the underlying mechanism that strain induced degradation of critical current density is of urgent importance to optimize the electromagnetic properties of superconducting polycrystals, thereby directly influencing the applications of corresponding magnets. At the macroscopic level, numerous models [10-15] have been developed to characterize strain dependence of critical current density of Nb₃Sn. However, the interpretation of measured results and proposed models remain, for a significant part, empirical, and lacking the connection to the underlying physics. At the microscopic level, Godeke *et al* [16] revealed the strain sensitivity of Nb₃Sn from the perspective of sub-lattice distortions. Note that the thermal fluctuations, vortex-vortex interactions and the interaction between the pinning force and quantized magnetic vortices driven by current determine the key electromagnetic properties of superconductors [17-24]. In polycrystalline superconductors such as Nb₃Sn and YBCO, grain boundaries (GBs) have been found to play a crucial role in vortex pinning. van der Laan *et al* [25] investigated the effects of strain and GB angle on the critical current density of YBCO GBs. Building on the strain energy of dislocation, Yue *et al* [26] studied the mechanisms of current transport in the [001]-tilt low-angle GBs, with results similar to the formula proposed by van der Laan *et al*. These studies for strain induced J_c degradation focus on the reversible stage and have not been associated with vortex behaviors. The effects of strain on the vortex pinning remain unclear and the mechanisms underlying the irreversible J_c degradation of polycrystalline superconductors induced by applied strain have yet to be fully elucidated.

In this paper, a multi-scale computational framework, that integrates a multi-scale mechanical model with a physical model, is introduced. Through the ‘reverse engineering’ of experimental J_c , we reveal the impact of strain on the superconductivity of grain boundaries and the associated vortex pinning for polycrystalline superconductors. Furthermore, without mechanical simulations, the internal damage can be approximated based on the electromagnetic experiments on J_c . Moreover, the J_c degradation of polycrystalline superconductor under

biaxial loads is analyzed by the computational framework.

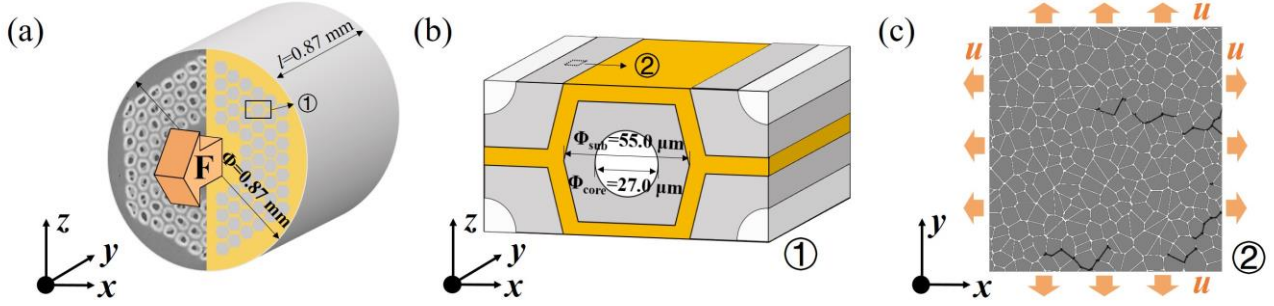


Fig. 1. (a) Schematic of the macroscopic model, where a IT Nb₃Sn wire exposed to a tensile mechanical load. (b) Schematic of the mesoscopic model, consists of several sub-elements and copper matrix. (c) Schematic of microscopic model, where a polycrystalline Nb₃Sn is subjected to displacements u from the mesoscopic model.

The most common experiments used to investigate the J_c degradation of polycrystalline superconductors like Nb₃Sn wire are the uniaxial quasi-static tensile tests. As shown in Fig. 1, in order to reproduce the mechanical response of Nb₃Sn wire, we consider a numerical model consisting of an internal tin (IT) Nb₃Sn wire. The wire with a length of 0.87 mm and a diameter of 0.87 mm, comprising a copper matrix and 108 sub-elements, is subjected to a tensile strain along the y -axis at a constant strain rate of 1×10^{-5} /s. To capture the damage evolution in polycrystalline Nb₃Sn, we develop a multi-scale framework consisting of macroscopic model, mesoscopic model and microscopic model. The mesoscopic model (Fig. 1(b)) consists of copper matrix and sub-elements with an average size of 55 μm . The microscopic model (Fig. 1(c)) consists of 2D polycrystalline Nb₃Sn with an area of $1.8 \times 1.8 \mu\text{m}^2$, where the average size of grains is 108 nm. The underlying idea of the multiscale model is that taking local displacements of higher-level model as inputs to analyze the mechanical response of lower-level model. With this method, we can simulate the mechanical responses of which ranges from polycrystalline Nb₃Sn to wire with acceptable computational resource.

To ensure the size of microscopic model is large enough to investigate the mechanical behavior and damage evolution of polycrystalline Nb₃Sn, four randomly selected polycrystalline Nb₃Sn (Panel 1 in Figs. 2(a-d)), which locate in different sub-elements, are considered. Panels 2-5 in Figs. 2(a-d) illustrates the damage evolution of the four samples with increasing applied strain. Previous experiments shown that the bare Nb₃Sn filament exhibits brittle fracture with applied loads [27]. However, for the fiber-matrix composite structure of Nb₃Sn wire, our simulation illustrates that polycrystalline Nb₃Sn exhibits progressive damage. One may argue it may be attributed to that the Nb₃Sn filaments are embedded in copper matrix. To deeply understand the

unexpected phenomenon, we present the numerical simulation for bare Nb₃Sn filament and fiber-matrix composite Nb₃Sn wire. The simulating results shown in Supplementary Information (SI) demonstrate the copper matrix with higher toughness limits the brittle fracture of Nb₃Sn. As further shown in Figs. 2(a-d), one can only observe intergranular fractures as the fracture strength of GBs is much lower than that of single grain [28].

Fig. 2(e) illustrates the elastic mechanical response of polycrystalline Nb₃Sn at the beginning stage of applying strain. However, with further increasing applied strain ($\epsilon_a > 0.37\%$), the local stress exceeds the fracture strength of GBs, resulting in crack occurrence and propagation along GBs (Panels 2-5 in Figs. 2(a-d)). Four samples exhibit very similar characteristics of the failure ratio of GBs, indicating that the simulated region is sufficiently large to eliminate the randomness of GB landscapes. In order to clearly capture the damage characteristics of polycrystalline Nb₃Sn, Fig. 2(f) presents the statistics of crack orientations at $\epsilon_a = 0.64\%$, where θ represents the included angle between the crack orientation and the x -axis. It can be clearly seen that cracks are most likely to propagate along GBs with small θ .

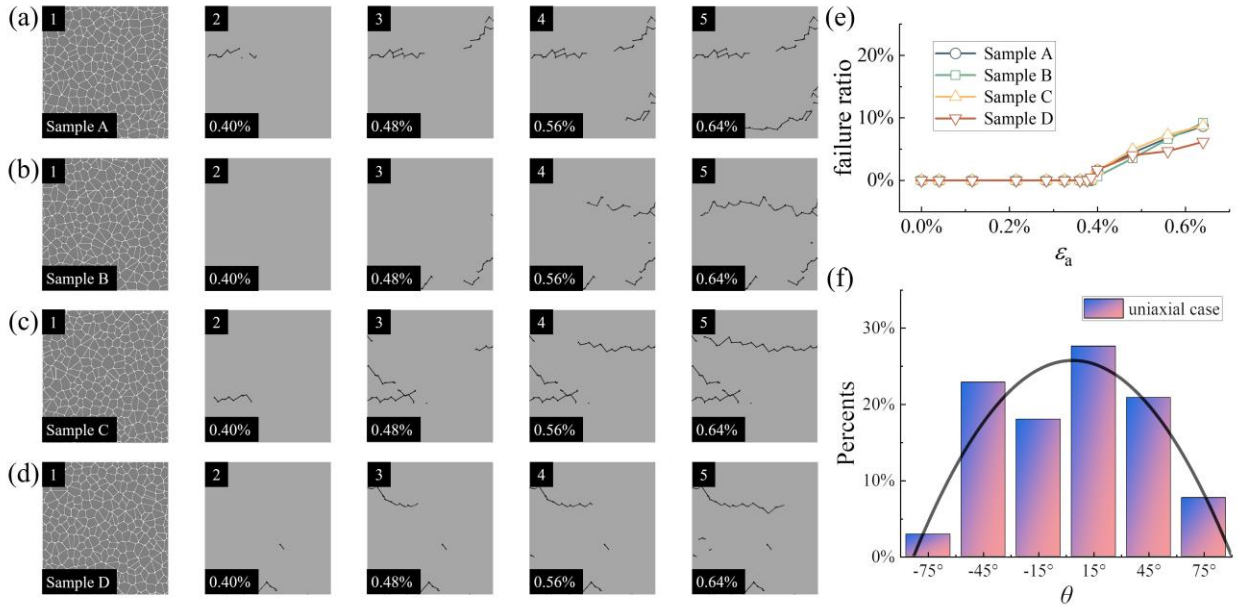


Fig. 2. (a-d) Four randomly selected samples and associated damage evolution with increasing applied strain ($\epsilon_a = 0.40\% \rightarrow 0.48\% \rightarrow 0.56\% \rightarrow 0.64\%$). (e) The failure ratio of GBs in four samples of polycrystalline Nb₃Sn versus strain. (f) Statistics of included angles at $\epsilon_a = 0.64\%$. Black line represents the fitting curve for the statistics results.

For typical experimental I_c - ϵ_a curves [8], we can clearly see two regions with different physical scenarios. One is the ‘elastic’ stage that the strain-induced J_c degradation is reversible and can recover to initial state after fully unloading. Another is the ‘plastic’ stage where J_c exhibits irreversible degradation. It is well known that the critical current density of superconductors is determined by the pinning force on magnetic vortices. For

polycrystalline Nb₃Sn, its pinning effect is primarily resulted from the suppressed superconductivity on GBs [5]. Experiments [29, 30] have demonstrated that stress/strain plays a significant role in Cooper pair formation at pinning center. Similar characteristics of J_c attenuation and mechanical response of polycrystalline Nb₃Sn with applied strain inspire us to reveal the underlying physical mechanism of strain-induced J_c degradation from the perspective of impact of strain on superconductivity of GBs and vortex pinning.

We propose a physical model to address the aforementioned problem based on time-dependent Ginzburg-Landau (TDGL) theory [31-33],

$$\frac{u}{\sqrt{1+\gamma^2|\psi|^2}}\left(\frac{\partial}{\partial t} + \frac{\gamma^2}{2}\frac{\partial|\psi|^2}{\partial t}\right)\psi = (\nabla - i\mathbf{A})^2\psi + [1-T-g(\mathbf{r})-|\psi|^2]\psi, \quad (1)$$

$$\frac{\partial\mathbf{A}}{\partial t} = \text{Re}[\psi^*(-i\nabla - \mathbf{A})\psi] - \kappa^2\nabla \times \nabla \times \mathbf{A}. \quad (2)$$

where ψ , \mathbf{A} and κ represent order parameter, vector potential and GL parameter, respectively. $g(\mathbf{r})$ describes the pinning landscape of GBs, which is non-zero at GBs and remains zero inside grains. Note that $u = \pi^4/14\zeta(3) \approx 5.79$, and the parameter $\gamma=10$ accounts for inelastic scattering of the superconductor. In our simulations, the polycrystalline Nb₃Sn with an area of $1.8 \times 1.8 \mu\text{m}^2$ is exposed to a magnetic field H_a , a transport current I_a and ambient temperature T . We use the magnetic field boundary conditions on the left and right borders, and periodic boundary conditions along the y -axis. The transport current along the y -axis is applied via the field boundary condition $H=H_a \pm H_1$, where H_1 represents the magnetic field induced by the current I_a . To efficiently simulate the vortex behaviors in the polycrystalline Nb₃Sn, a stable implicit numerical algorithm for TDGL theory implemented on GPU is introduced in Ref. [34].

Experiments indicated that, with different mechanical loading modes, invariant strain function [13, 35] gives a more unified analytical treatment of strain dependence of critical properties of Nb₃Sn tapes in reversible regions. In order to obtain a general formula for the impact of strain on superconductivity of GBs, we use a function with an independent variable of the second invariant of strain tensor J_2 . In our physical model, investigating the effects of strain on J_c requires the superconductivity of GBs at zero strain state ($|\psi_{\text{GB}0}|$). However, to date, the value of $|\psi_{\text{GB}0}|$ of polycrystalline Nb₃Sn measured by experiments has not been reported. Therefore, a series of $|\psi_{\text{GB}0}|$ (0.90, 0.80, 0.75, 0.65, 0.60, 0.50 and 0.40) are selected in the TDGL simulations. In the following text, we take one $|\psi_{\text{GB}0}|$ to introduce our physical model.

For the case with $|\psi_{\text{GB}0}|=0.75$, the impact of strain on $|\psi_{\text{GB}}|$ is obtained through the ‘reverse engineering’ method by tuning $|\psi_{\text{GB}}|$ to reproduce the experimental data of J_c - ε_a . Fig. 3(a) illustrates the experimental J_c - ε_a

and associated simulated results. The critical current density decreases monotonically with increasing applied strain. For the polycrystalline Nb₃Sn in ‘elastic’ stage, where no cracks occur, the degradation of J_c is solely determined by strain-induced suppression of $|\psi_{GB}|$ (points A, B, C and D in Fig. 3(a)). This suppression is reversible and can recover to its initial state after unloading. Once ε_a exceeds ε_{ir} , the blue line illustrates the J_c degradation induced by reversible strain and cracks (points E, F, G and H in Figs. 3(a)). In contrast, if we only consider the effect of reversible strain on $|\psi_{GB}|$, corresponding J_c attenuation of Nb₃Sn is shown by the yellow line. In the irreversible stage, there exist significant differences between experiments and the simulated results without considering damage. It indicates that the damage of polycrystalline Nb₃Sn gradually dominates in J_c degradation with further increasing ε_a . Besides, the strain-induced cracks are not recoverable, resulting in the irreversible degradation of J_c . Surprisingly, the simulated J_c after partial unloading (points E', F', G' and H' in Figs. 3(a)) is in good agreements with corresponding experimental results, providing clear evidence for the validation of the multi-physics computational framework.

The results of the case with other $|\psi_{GB0}|$ can be obtained by the similar procedure as $|\psi_{GB0}|=0.75$. Fig. 3(b) illustrates the experimental J_c - ε_a and simulated J_c degradation with $|\psi_{GB0}|=0.40$. For the cases with $|\psi_{GB0}|\geq 0.80$, the simulated results indicate that J_c - ε_a exhibits non-monotonicity with tensile strain, which is not consistent with experimental results [8] (see more details in SI). For the case with $|\psi_{GB0}|\leq 0.40$, there exist deviation between experimental and simulated J_c with increasing applied strain, indicating that small $|\psi_{GB0}|$ cannot reproduce the experiments [8]. Another evidence [36] also demonstrated that the simulation with $|\psi_{GB0}|\leq 0.40$ cannot reproduce the experimental J_c of Nb₃Sn well, where J_c can be enhanced with increasing grain size at high fields. Therefore, the reasonable value of $|\psi_{GB0}|$ should be in the scopes from 0.40 to 0.75. Fig. 3(c) represents the $|\psi_{GB}|-J_2^{0.5}$ curves for different $|\psi_{GB0}|$ of 0.75, 0.60 and 0.40 obtained through the ‘reverse engineering’ method. The superconductivity of GBs decrease with increasing applied strain and three $|\psi_{GB}|-J_2^{0.5}$ curves exhibit similar trends with each other.

For a given applied current, panel 3 of Figs. 3(e) show that no continuous vortex motion occurs in the case without applied loads, indicating that the applied Lorentz force is not sufficiently large to move the vortices along the GBs or drag the vortices out of the GBs. However, as applied strain is increased to 0.13%, the vortex motion is observed, especially along the GBs whose included angle is around 0° (Panels 4-6 of Fig. 3(e)). It is attributed to the fact that the strain suppresses the Cooper pair formation at GBs, thereby reducing the pinning effects. As ε_a exceeds the irreversible strain, cracks initiate and propagate along GBs. Panels 7-8 of Fig. 3(e)

illustrate that cracks act as flux flow channels and promote the vortex motion.

As a matter of fact, our physical model can be used to approximate the damage of superconducting polycrystals according to the electromagnetic response and thus the mechanical simulations are not necessary, especially for the internal damage of wire that cannot be directly observed by SEM experiments. For a Nb_3Sn wire, the J_c degradation with a given stress/strain state can be obtained by transport measurements. Meanwhile, numerical simulations for polycrystalline Nb_3Sn without considering damage are carried out to determine the critical current density. As shown in Fig. 3(d), the difference between two results roughly reflects the damage evolution of Nb_3Sn wire, which increase with applied strain and exhibits similar characteristics with the failure ratio of GBs illustrated in Fig. 2(e).

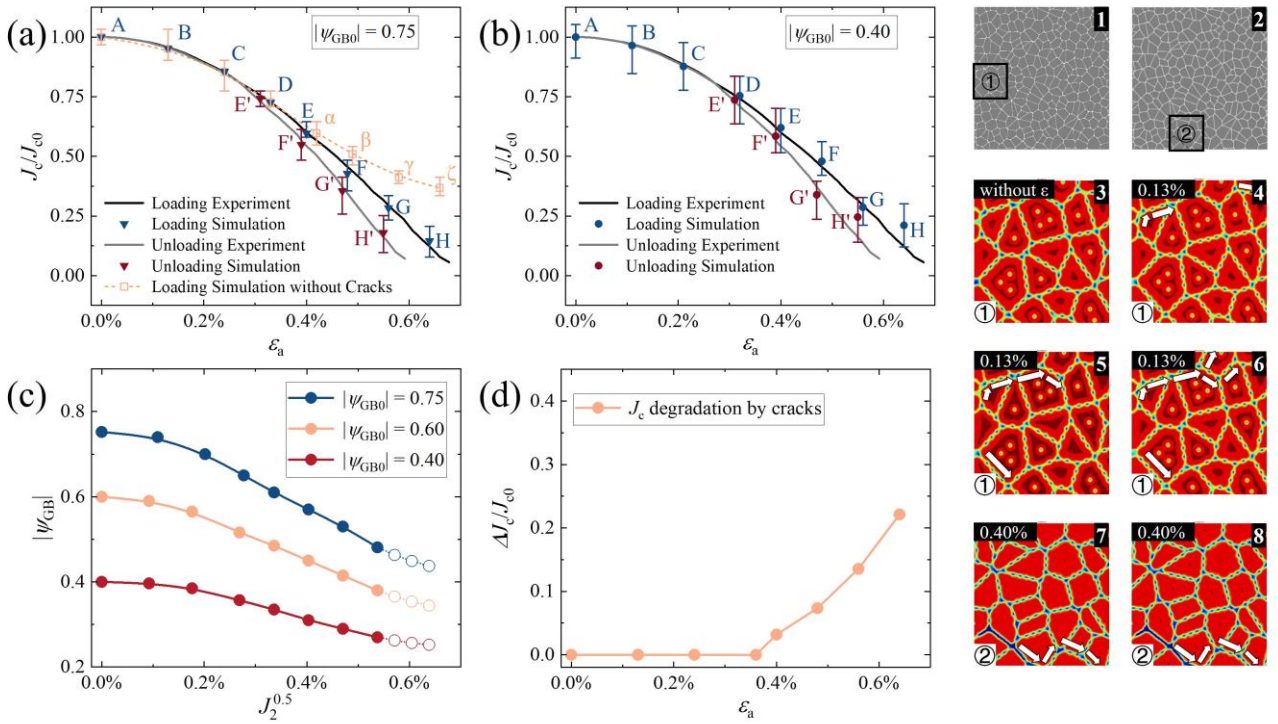


Fig. 3. (a-b) Black solid line and gray solid line represent the experimentally measured J_c - ϵ_a under loading and partial unloading, respectively. Blue solid symbols and red solid symbols represent the average simulated J_c for four samples under loading and partial unloading. The yellow empty symbols in (a) represent the average simulated J_c and without consideration of cracks. (c) ψ_{GB} as a function of $J_2^{0.5}$ with different ψ_{GB0} (0.75, 0.60 and 0.40). Dashed lines represent the extended data. (d) J_c degradation caused by cracks. (e) Panels 1-2 refer to the damage of Sample B without and with damage. Panels 3-8 indicate the corresponding vortex behaviors at different moments. The white arrows represent the paths of vortex motion.

Through the experimental J_c degradation under uniaxial tensile loads, we confirm the validation of the

proposed computational framework. Unlike the uniaxial loading condition, superconducting magnets are subjected to complicated Lorentz force during the current ramping process. Accurately understanding the J_c degradation under complicated loads is crucial for the property evaluation of superconductors and stable operation of electromagnets. In the following text, we explore the characteristics of mechanical behaviors and strain dependent J_c of Nb_3Sn wire for biaxial case.

We consider a representative volume element (RVE) of a typical Nb_3Sn magnet. Fig. 4(a) illustrates the RVE with length of 0.95 mm and cross section area of $0.95 \times 0.95 \text{ mm}^2$, consisting of an IT Nb_3Sn wire and surrounding epoxy. The RVE is subjected to a biaxial load, i.e., an applied compressive strain along the x -axis and an applied tensile strain along the y -axis. Fig. 4(b) illustrates the average maximum principal stress σ_a^p and the maximum principal stress σ_{\max}^p versus $J_2^{0.5}$. σ_a^p increase linearly with the $J_2^{0.5}$ and reaches a peak of 164 MPa. The damage initiates at $J_2^{0.5}=0.33\%$ and the maximum principal stress exists intensive jumps occur as J_2 further increases (subgraph in Fig. 4(b)), attributed to the concentrated crack initiations and propagations. Fig. 4(c) demonstrates the damage evolutions of polycrystalline Nb_3Sn under biaxial loads at $J_2=0.33\%$, 0.37% , 0.46% , and 0.52% . Unlike the uniaxial tensile cases, cracks prefer orienting at $\theta = \pm 45^\circ$ with $J_2=0.52\%$ (Panels 1-5 of Fig. 4). It indicates that the mechanical behaviors and damage evolutions of polycrystalline Nb_3Sn depend strongly on the mechanical loading modes.

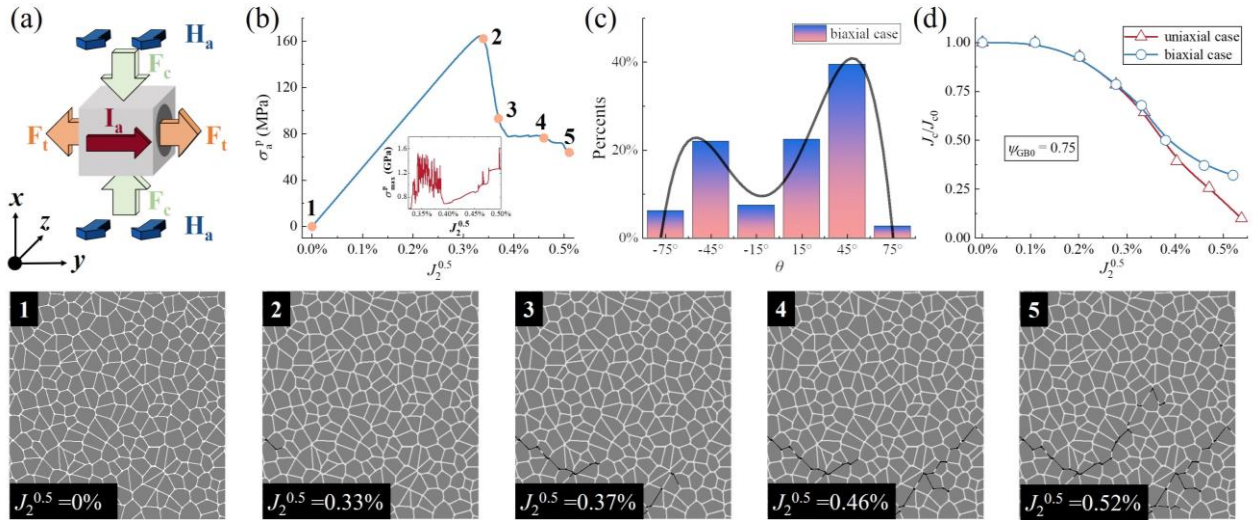


Fig. 4. (a) Schematic of a RVE of Nb_3Sn magnet exposed to a transport current I_a , an external magnetic field H_a , and a biaxial mechanical load. (b) the average maximum principal stress σ_a^p (blue line) and the maximum principal stress σ_{\max}^p (red line) versus $J_2^{0.5}$. (c) The statistics of crack orientations at $J_2^{0.5}=0.52\%$. Black line represents the fitting function for

the statistics results. (d) The simulated J_c - $J_2^{0.5}$ curves for uniaxial (red line) and biaxial (blue line) cases. (e) Damage evolutions of polycrystalline Nb₃Sn with different strains ($J_2^{0.5}=0\% \rightarrow 0.33\% \rightarrow 0.37\% \rightarrow 0.46\% \rightarrow 0.52\%$).

Fig. 4(d) illustrates the strain dependence of critical current density for biaxial and uniaxial cases. In the reversible stage ($J_2^{0.5} < 0.33\%$), the J_c degradation under biaxial loads show good agreements with that under uniaxial tensile loads. The consistent degradation of critical properties versus $J_2^{0.5}$ under different mechanical loading conditions is also reported in Ref. [35]. However, as the strain exceeds the irreversible strain, there exists obvious difference in J_c degradation between uniaxial and biaxial cases, suggesting J_c attenuation is strongly dependent on the mechanical loading modes. It is attributed to the fact that the significant difference of crack orientations leads to distinct critical vortex depinning of vortices.

In conclusion, we proposed a multi-scale computational framework integrating a multi-scale mechanical model with a physical model. The validation of the computational framework is confirmed through the experimental J_c degradation with uniaxial tensile loads. The impact of strain on superconductivity and vortex pinning of polycrystalline superconductors is revealed. The irreversible J_c degradation of polycrystalline superconductors is mainly attributed to the suppression of vortex pinning induced by both reversible strain and irreversible damage. The most striking finding is that, without mechanical simulations, the proposed physical model can be utilized to approximate the internal damage of superconducting polycrystals based on the electromagnetic experiments on J_c . Finally, we explore the J_c degradation of polycrystalline superconductors subjected to biaxial loads by the computational framework. Our findings indicate that the irreversible J_c degradation is strongly dependent on the mechanical loading modes. The computational framework paves the way for mechanical tuning superconductivity and associated vortex pinning, and exploring the damage of superconducting polycrystals through electromagnetic responses.

Acknowledgements—We acknowledge support by the National Natural Science Foundation of China (Grant No. 12372210). We also acknowledge support by the Fundamental Research Funds for the Central Universities lzujbky-2024-jd zx02. We thank for the helpful discussions in mechanical analysis of polycrystalline structures by He Ding at North university of China.

Reference

- [1] N. Mitchell, Finite element simulations of elasto-plastic processes in Nb₃Sn strands, *Cryogenics*, 45 (2005) 501-515.
- [2] M.C. Jewell, P.J. Lee, D.C. Larbalestier, The influence of Nb₃Sn strand geometry on filament breakage

- under bend strain as revealed by metallography, *Superconductor Science and Technology*, 16 (2003) 1005.
- [3] S. Hahn, K. Kim, K. Kim, X. Hu, T. Painter, I. Dixon, S. Kim, K.R. Bhattarai, S. Noguchi, J. Jaroszynski, D.C. Larbalestier, 45.5-tesla direct-current magnetic field generated with a high-temperature superconducting magnet, *Nature*, 570 (2019) 496-499.
- [4] Y.H. Zhou, C. Liu, L. Shen, X. Zhang, Probing of the internal damage morphology in multilayered high-temperature superconducting wires, *Nat. Commun.*, 12 (2021) 3110.
- [5] X. Xu, A review and prospects for Nb₃Sn superconductor development, *Supercond. Sci. Technol.*, 30 (2017) 093001.
- [6] Muller C B and Saur E 1963 *Adv. Cryog. Eng.* 8 574.
- [7] Buehler W and Levinstein H J 1965 *J. Appl. Phys.* 36 3856.
- [8] N. Cheggour, T.C. Stauffer, W. Starch, L.F. Goodrich, J.D. Splett, Implications of the strain irreversibility cliff on the fabrication of particle-accelerator magnets made of restacked-rod-process Nb₃Sn wires, *Scientific Reports*, 9 (2019).
- [9] C. Xue, H.-X. Ren, P. Jia, Q.-Y. Wang, W. Liu, X.-J. Ou, L.-T. Sun, A.V. Silhanek, Holistic numerical simulation of a quenching process on a real-size multifilamentary superconducting coil, *Nat Commun* (Accepted), (2024).
- [10] J.W. Ekin, Strain scaling law for flux pinning in practical superconductors. Part 1: Basic relationship and application to Nb₃Sn conductors, *Cryogenics*, 20 (1980) 611-624.
- [11] S. Oh, K. Kim, A scaling law for the critical current of Nb₃Sn stands based on strong-coupling theory of superconductivity, *Journal of Applied Physics*, 99 (2006).
- [12] D.M.J. Taylor, D.P. Hampshire, Relationship between then-value and critical current in Nb₃Sn superconducting wires exhibiting intrinsic and extrinsic behaviour, *Superconductor Science and Technology*, 18 (2005) S297-S302.
- [13] B.t. Haken, A. Godeke, H.H.J.t. Kate., The Influence of Compressive and Tensile Axial Strain on the Critical Properties of Nb₃Sn Conductors, *IEEE Trans. Appl. Supercond.*, 5 (1995) 1909.
- [14] B. Bordini, P. Alknes, L. Bottura, L. Rossi, D. Valentinis, An exponential scaling law for the strain dependence of the Nb₃Sn critical current density, *Superconductor Science and Technology*, 26 (2013).
- [15] X.F. Lu, D.P. Hampshire, The field, temperature and strain dependence of the critical current density of a powder-in-tube Nb₃Sn superconducting strand, *Supercond. Sci. Technol.*, 23 (2010) 025002.
- [16] A. Godeke, F. Hellman, H.H.J.t. Kate, M.G.T. Mentink, Fundamental origin of the large impact of strain on superconducting Nb₃Sn, *Superconductor Science and Technology*, 31 (2018).
- [17] C. Reichhardt, N. Grønbech-Jensen, Collective Multivortex States in Periodic Arrays of Traps, *Physical Review Letters*, 85 (2000) 2372.
- [18] D. Ray, C.J. Olson Reichhardt, B. Janko, C. Reichhardt, Strongly enhanced pinning of magnetic vortices in type-II superconductors by conformal crystal arrays, *Phys. Rev. Lett.*, 110 (2013) 267001.
- [19] L. Embon, Y. Anahory, Ž.L. Jelić, E.O. Lachman, Y. Myasoedov, M.E. Huber, G.P. Mikitik, A.V. Silhanek, M.V. Milošević, A. Gurevich, E. Zeldov, Imaging of super-fast dynamics and flow instabilities of superconducting vortices, *Nature Communications*, 8 (2017).
- [20] C. Reichhardt, C.J. Olson, F. Nori, Dynamic Phases of Vortices in Superconductors with Periodic Pinning, *Phys. Rev. Lett.*, 78 (1997) 2648.
- [21] C. Reichhardt, C.J. Olson, F. Nori, Nonequilibrium dynamic phases and plastic flow of driven vortex lattices in superconductors with periodic arrays of pinning sites, *Phys. Rev. B*, 58 (1998) 6534.
- [22] O.M. Auslaender, L. Luan, E.W.J. Straver, J.E. Hoffman, N.C. Koshnick, E. Zeldov, D.A. Bonn, R. Liang, W.N. Hardy, K.A. Moler, Mechanics of individual isolated vortices in a cuprate superconductor, *Nature Physics*,

5 (2008) 35-39.

- [23] J. Jiang, M.V. Milošević, Y.-L. Wang, Z.-L. Xiao, F.M. Peeters, Q.-H. Chen, Field-Free Superconducting Diode in a Magnetically Nanostructured Superconductor, *Physical Review Applied*, 18 (2022).
- [24] Y.Y. Lyu, J. Jiang, Y.L. Wang, Z.L. Xiao, S. Dong, Q.H. Chen, M.V. Milosevic, H. Wang, R. Divan, J.E. Pearson, P. Wu, F.M. Peeters, W.K. Kwok, Superconducting diode effect via conformal-mapped nanoholes, *Nat. Commun.*, 12 (2021) 2703.
- [25] D.C. van der Laan, T.J. Haugan, P.N. Barnes, Effect of a Compressive Uniaxial Strain on the Critical Current Density of Grain Boundaries in Superconducting $\text{YBa}_2\text{Cu}_3\text{O}_{7-\delta}$ Films, *Physical Review Letters*, 103 (2009).
- [26] D.-H. Yue, X.-Y. Zhang, J. Zhou, Y.-H. Zhou, Current transport of the [001]-tilt low-angle grain boundary in high temperature superconductors, *Appl. Phys. Lett.*, 103 (2013) 232602.
- [27] M.T. Dylla, S.E. Schultz, M.C. Jewell, Fracture Strength Distribution of Individual Nb_3Sn Filaments, *IEEE Transactions on Applied Superconductivity*, 26 (2016) 1-7.
- [28] Z. Liu, B. Wang, Comparative study on the strain-dependent mechanical and electronic properties of Nb_3Al and Nb_3Sn , *Materials Research Express*, 8 (2021).
- [29] A. Llordes, A. Palau, J. Gazquez, M. Coll, R. Vlad, A. Pomar, J. Arbiol, R. Guzman, S. Ye, V. Rouco, F. Sandiumenge, S. Ricart, T. Puig, M. Varela, D. Chateigner, J. Vanacken, J. Gutierrez, V. Moshchalkov, G. Deutscher, C. Magen, X. Obradors, Nanoscale strain-induced pair suppression as a vortex-pinning mechanism in high-temperature superconductors, *Nat. Mater.*, 11 (2012) 329-336.
- [30] A. Kremen, S. Wissberg, N. Haham, E. Persky, Y. Frenkel, B. Kalisky, Mechanical Control of Individual Superconducting Vortices, *Nano. Lett.*, 16 (2016) 1626-1630.
- [31] L. Kramer, W.-T. R. J, Theory of Dissipative Current-Carrying States in Superconducting Filaments, *Physical Review Letters*, 40 (1978) 15.
- [32] G.R. Berdiyrov, M.V. Milosevic, M.L. Latimer, Z.L. Xiao, W.K. Kwok, F.M. Peeters, Large magnetoresistance oscillations in mesoscopic superconductors due to current-excited moving vortices, *Phys. Rev. Lett.*, 109 (2012) 057004.
- [33] G. Berdiyrov, K. Harrabi, F. Oktasendra, K. Gasmı, A.I. Mansour, J.P. Maneval, F.M. Peeters, Dynamics of current-driven phase-slip centers in superconducting strips, *Physical Review B*, 90 (2014).
- [34] Q.-Y. Wang, C. Xue, Stable implicit numerical algorithm of time-dependent Ginzburg–Landau theory coupled with thermal effect for vortex behaviors in hybrid superconductor systems, *Superconductor Science and Technology*, 37 (2024).
- [35] W.D. Markiewicz, Comparison of strain scaling functions for the strain dependence of composite Nb_3Sn superconductors, *Supercond. Sci. Technol.*, 21 (2008) 054004.
- [36] H.-X. Ren, C. Xue, Improving critical current density of Nb_3Sn by optimizing pinning potential of grain boundary and grain size, *Superconductor Science and Technology*, 35 (2022).